MedCrave
Step into the World of Research
Journal of Applied Biotechnology and Bioengineering

Research Article

Open Access

Hierarchical self-assembly in ionic liquid crosslinked polyelectrolyte gels as a citric acid sensor

Abstract

The design of an enzyme-free biocompatible electrochemical platform for the detection of citric acid is discussed. We have studied sol-gel transition in DNA ionic liquid solution triggered by the ionic liquid (IL), (1-Octyl-3-methylimidazolium Chloride [C8mim][Cl]; concentration= 0.1 to 1.0% (w/v)). Rheology and Small-angle neutron scattering (SANS) studies characterized their viscoelastic and microstructural properties. The gel modulus was found to vary from 10 to 60 Pa concomitant with a tunable temperature of gelation. SANS data yielded the persistence length of DNA (50 ± 12 nm) and the mesh size of these gels (ξ = 2.5±0.5 nm). Remarkably, this ionogel served as an excellent electrochemical sensor for citric acid detection in the application window of 0.02-0.08 mM analyte concentration with a detection limit of 1.5×10^{-8} molL^{-1}. Yet another non-trivial application of the versatile DNA gel is demonstrated here.

Keywords: ionic liquid, DNA, rheology, SANS, electrochemical sensor

Volume 9 Issue 5 - 2022

Pankaj Kumar Pandey,[1] Kamla Rawat,[2] VK Aswal,[3] J Kohlbrecher,[4] Himadri B Bohidar[1]
[1]School of Physical Sciences, Jawaharlal Nehru University, India
[2]Department of Chemistry, School of Chemical and Life Science, India
[3]State Physics Division, Bhabha Atomic Research Centre, India
[4]Laboratory for Neutron Scattering, Paul Scherrer Institut, Switzerland

Correspondence: Himadri B Bohidar, School of Physical Sciences, Jawaharlal Nehru University, New Delhi, India, Email bohidarjnu@gmail.com
Kamla Rawat, Department of Chemistry, School of Chemical and Life Science, Jamia Hamdard, New Delhi, India, Email kamlarawat@jamiahamdrad.ac.in

Received: September 08, 2022 | **Published:** September 19, 2022

Abbreviations: DNA, deoxyribonucleic acid; EGDA, ethylene glycol diacrylate; IL, ionic liquid

Introduction

Deoxyribonucleic acid, DNA being a highly functional molecule with excellent structural versatility, its derivatives like hydrogels, interpolymer complexes, condensates, etc. have continued to draw much attention which is evident from the following examples. The behavior of pH-triggered fast responding DNA hydrogel was demonstrated for sustainability under different pH conditions, which is required for the tailored application of this gel in biology, in particular.[1] Different length of DNA chains have been shown to form a stable assembly with cationic colloidal particles.[2] Graphene oxide was used to form multifunctional DNA hydrogel with high rigidity, biocompatibility, and self-healing property.[3] Supramolecular polypeptide -DNA hydrogel with high rigidity modulus was used for 3D printing.[4] DNA is polyanionic in nature and the double helix strands repel each other because of Coulombic repulsion. Therefore, to facilitate physical entanglement a cross-linker such as ethylene glycol diacrylate (EGDA) is often used.[5] Polymerase enzyme-based DNA meta-hydrogel could be used in electrical circuits in which water played the role of an ON-OFF switch.[6] Interaction of DNA and multi-walled carbon nanotube leads to the formation of self-assembled DNA-hybrid hydrogel.[7] Comparative interaction study of ds- and ss-DNA with cation was extensively explored and it was concluded that ss-DNA collapsed more than the other.[8] DNA functionalized hydrogel was successfully used to detect mercury from the environment.[9] Stable DNA hydrogel fibers could be prepared in the presence of ionic liquid without requiring high temperature.[10] Surfactant CTAB, and lysozyme protein enabled the assembly of DNA gel particles with *ss*- or *ds*-DNA.[11] DNA hydrogel was shown to entrap gold nanoparticles inside its network.[12] Strain hardening was noticed in both chemical and physical DNA gels at 40 % deformation.[13] Cross-linking of DNA gel with organic salt such as $CaCl_2$ showed reduced osmotic pressure.[13] Relaxation dynamics and rheological properties of DNA hydrogels were systematically explored and microscopic changes were probed by neutron scattering technique.[15,16]

On the other hand, gelation in ionic liquid solutions is not uncommon. Sui et al have shown that poly(ferrocenylsilane) in the presence of polyionic liquid forms nanogels.[17] It was seen that block copolymer forms self-assembled spherical or worm-like micelles in ionic liquid.[18] Ionic liquid-based biopolymer gels typically have very high viscosity and melting temperature. Further, enabled by hydrophobic hydration, polymers like cellulose, which is generally insoluble in water and most other solvents, can be dissolved in ionic liquids.[19] Even at very low concentration of DNA gelation was sustained in ionic liquid solutions.[20] Self-assembly of the triblock copolymer was studied with the help of rheology and it was found that gels formed in the presence of ionic liquid were stable even at higher temperatures (100 ^{0}C).[21] Pandey et al have demonstrated the formation of DNA ionogels and studied their time-dependent structural dynamics, viscoelastic properties and microscopic structures.[22] These ionogels have found applications in the production of lithium-ion batteries, fuel cells, solar cells, electrochemical sensors, actuators and also as drug encapsulation and release vehicles.[23] Herein, we have studied 1-octyl-3 methylimidazolium ionic liquid-based DNA ionogels and these have been used to propose an electrochemical biosensor for the important nutrient citric acid. This is a weak organic acid with molecular formula $C_6H_8O_7$.

Material and methods

2000 base pair Deoxyribonucleic acid (DNA), sodium salt from Salmon testes (Catalog no. D1626) and the ionic liquid (IL) 1-octyl-3-methyl imidazolium chloride [C8mim][Cl] were purchased from Sigma-Aldrich (USA). Potassium ferrocyanide, $K_4Fe(CN)_6$ and Potassium ferricyanide, $K_3Fe(CN)_6$ were purchased from SRL (India). Potassium Chloride and KCL were from CDH (India) and so were the analytes Cholesterol (Chox), Citric acid (CA) and Gallic acid (GA). Urea (U) and Dextrose (Dex) were purchased from Loba Chemie (India). Oxalic acid (OA) was purchased from RANKEM (India). Indium-tin-oxide (ITO, 1.1 mm thick and 25 Ω sq^{-1} resistance) substrate was purchased from Balzers, UK (Baltracom 247 ITO). All measurements were performed at room temperature 25^0 C unless otherwise stated.

DNA was dissolved in different concentration (0.1% to 1.0 % (w/v)) of ionic liquid aqueous solutions in such a way that final concentrations of DNA remained fixed at 1% (w/v) in all the samples. These samples were heated to 90 ^{0}C and maintained at that temperature for 30 min. Then, on cooling to room temperature optically clear gel samples were obtained. Since, these gels were made in ionic liquid solutions, these are being referred to as ionogels.

Viscoelastic properties of ionogels were measured by AR 500 Rheometer, TA Instruments, (England) using a 20 mm and 2^0 cone-plate geometry. Small angle neutron scattering (SANS) measurement was carried out at the Swiss Spallation Neutron Source SINQ, PSI (Switzerland) facility using beam wavelength of 0.8 nm.[24] Electrochemical sensing of different analytes was performed on a cyclic voltammeter (CV) on Auto lab Potentiostat/ Galvanostat (Eco Chemie, Netherlands).

The thin film of DNA ionogel-ITO electrode was prepared by the drop casting method, where a drop of the ionosol was uniformly coated by dispersion of 50 µl of the suspension onto an ITO plate that had a covered surface area of 0.25 cm^2 which created a thin gel film. The films were then allowed to dry at room temperature for about 24 hours. The electrochemical behaviour of the prepared electrodes was monitored and the maximum current was detected for the sample with ionic liquid concentration of 0.7% (w/v). Except for a few experiments (standardization of IL concentration) all other experiments were performed on thin gel films containing 1% (w/v) DNA and 0.7% (w/v) IL.

Results

Viscoelastic behavior

Rheological characterization of the samples were performed by following two distinct protocols:[25,26] (i) isothermal frequency sweep studies where dispersion behavior of storage G' and loss modulus G'' were recorded (Figure 1a), and (ii) isochronal temperature sweep studies that yielded the melting profile of the gels (Figure 2a). The photograph of these samples is shown in Figure 1b which shows that the meniscus of the gel does not flow upon inversion of the test tube. In the linear viscoelastic regime the dependence of elastic modulus on frequency ω is often given by the power-law relation [27,28]

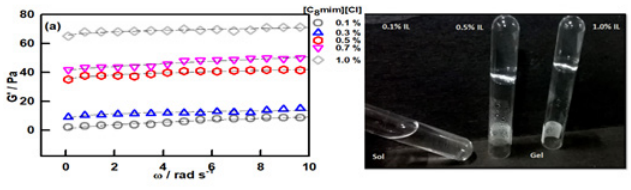

Figure 1 (a) Frequency-dependent behaviour of storage modulus G' with different IL concentration and (b) photograph of sol and ionogels.

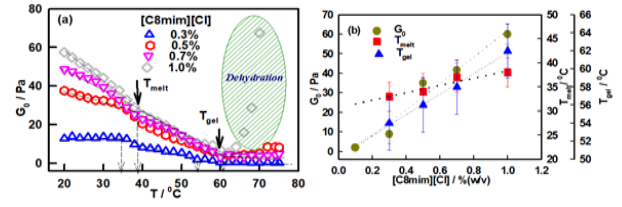

Figure 2 (a) Temperature-dependent profile for storage modulus G_0. Change in slope depicts the transition temperature, referred as T_{melt} and T_{gel}. (b) IL concentration-dependent variation of G_0, T_{melt} and T_{gel}.

$$G'(\omega) \sim \omega^n \quad (1)$$

Least squares fitting of the data to above equation yields the exponent n = 0.8 ± 0.4 (Figure S1 (Electronic Supporting Information)). The characteristic exponent n lies between 0 and 2 and uniquely defines the viscoelasticity of the material. When n = 0, it refers to a Hookean solid whereas n = 2 corresponds to a Maxwellian viscoelastic material. The gel strength G_0 can be determined from

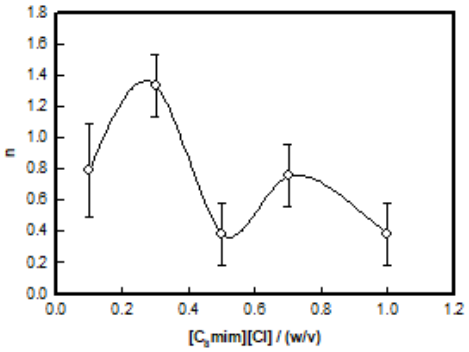

Figure S1 Variation of power-law exponent obtained from frequency sweep rheology data.

$$G_0 = lim_{\omega \to 0} G'(\omega) \quad (2)$$

The value of G_0 changed from 10 ± 4 to 60 ± 10 Pa with increase in the IL concentration from 0.1% to 1.0% (w/v). Therefore, as IL concentration was raised there was a concomitant increase in the gel rigidity indicating the formation of a denser network (Figure 1).

A characteristic length scale called the viscoelastic length ξ_{el} can be deduced from the knowledge of G_0. The elastic energy stored in the network of volume ξ_{el}^3 is equal to the thermal energy for an equilibrium gel. Hence, ξ_{el} is given by[29]

$$\xi_{el} = \sqrt[3]{\frac{K_B T}{G_0}} \quad (3)$$

For the 0.1% IL sample ξ_{el} = 120 nm which reduced to 40 nm for 1.0 % IL sample (Figure S2 (Electronic Supporting Information) implying formation of high network density gels in sols that had a propensity of ionic liquids. Higher network density would mean a stronger gel which is depicted in Figure 2b.

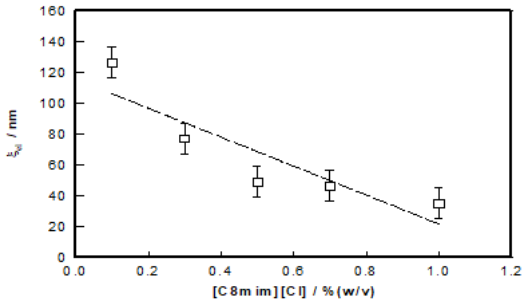

Figure S2 Variation of viscoelastic length obtained from G_0.

The isochronal temperature sweep data of these gels clearly show two transition temperatures which are marked in Figure 2(a). The

Citation: Pandey PK, Rawat K, Aswal VK, et al. Hierarchical self-assembly in ionic liquid crosslinked polyelectrolyte gels as a citric acid sensor. *J Appl Biotechnol Bioeng.* 2022;9(5):142–147. DOI: 10.15406/jabb.2022.09.00302

first transition point was found between temperatures 35-40 ^{0}C (T_{melt}) whereas the second was located (T_{gel}) in the higher temperature region (53-62 ^{0}C)**.** The dependence of T_{melt} and T_{gel} on ionic liquid content is shown in Figure 2(b).

Note that the gel melting starts at T_{melt} and ends at T_{gel}. From Figure 2 (b), it can be easily interpreted that all G_0, T_{melt} and T_{gel} are linearly dependent with IL concentration**.** The gelation is associated with enthalpy change conforming to the first order phase transition behaviour. Linear fitting of G_0, T_{melt} and T_{gel} data with respect to IL concentration, shows the change in these parameters per unit change in IL concentration (slope of the fitting line) is given by G_0 = 67.16 Pa/ % (w/v), T_{melt} = 7.66 ^{0}C/ % (w/v), and T_{gel} = 11.40 ^{0}C/ % (w/v). Hence, this ionogel can be a designated as a tunable gel where the gelation temperature can be tuned in the range of typically ~ 50 to 65^0 C which is remarkable for a biopolymer gel. This is a much sought after property in the design of encapsulation and release vehicles in drug delivery formulations.

Small angle neutron scattering (SANS)

The microscopic structure of ionogel was probed by small angle neutron scattering measurement. The I(q) vs q structure factor data is shown in Figure 3. The data was defined in two distinct regions decided by $\frac{1}{I} vs\, q^2$ and $\frac{1}{\sqrt{I}} vs\, q^2$ protocols. These two regions were best fitted by Guinier law and Ornstein-Zernike (OZ) law.[22] Guinier law was applied to the low-q region ($qR_g < 1$), where R_g stands for the radius of gyration for the biopolymer. For the intermediate-q region, OZ function was applied for data fitting. The OZ equation describes the scattering from the dynamic network associated with the inter-chain overlap (i.e. the dynamic component). Therefore, yields the distance between two adjutant overlaps which is also called mess size (ξ) for the associated network. The low-q region (0.0552 Å^{-1} ≤ q ≤ 0.1173) was best fitted to the Guinier description and the intermediate-q region (0.0180 ≤ q ≤ 0.2480) to the OZ function. Therefore,

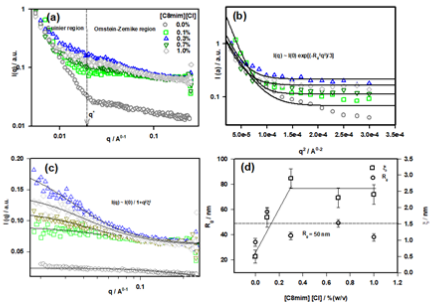

Figure 3 (a) I(q) vs q structure factor profile of different ionogels, (b) structure factor profile for low-q region fitted to Guinier function, (c) intermediate-q region fitted to OZ function and, (d) variation of parameters R_g and ξ with ionic liquid concentration.

$$I(q) = I_G exp(-(R_g^2 q^2)/3) + \frac{I_{OZ}}{1 + q^2\,\xi^2} \qquad (4)$$

The first two terms of the above equation correspond to Guinier and Ornstein-Zernike function, respectively. In eqn. (4) I_G and I_{OZ} are q-independent pre-factors. R_g denotes the radius of gyration for the polymer and ξ is corresponding to correlation length or mess size of the gel network. The boundary between two regions is defined by a cross-over wave vector q* value (Figure 3a).

Form the data fitting, we obtained the value of R_g is 50 ± 12 nm which corresponds to the persistence length of DNA (~50 nm)[30,31] and value of the mesh size was ξ = 2.5 ± 0.5 nm. The variation of these with ionic liquid concentration is shown in Figure 3d. The crossover wave vector q^* was 0.019 $Å^{-1}$ leading to a cross-over length ($L^* = 2\pi/q^*$) of 33 nm sample (Figure S3 (Electronic Supporting Information).

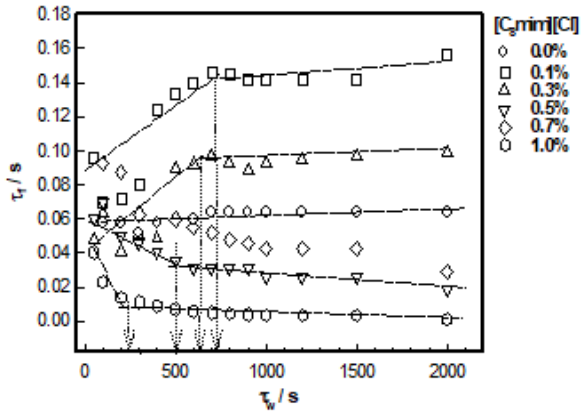

Figure S3 Plots of relaxation time of fast modes with waiting time, t_w shown for different IL concentrations.

Electrode characterization

The DNA Ionogel/ITO electrodes were characterized by Fourier transform infrared spectroscopy (FTIR) in the frequency range of 400 – 4000 cm^{-1} to investigate the changes that occurred after binding to the citric acid (Figure 4). We analyzed this on the basis in the variation in peak intensity. The DNA Ionogel/ITO electrode showed a broad peak located at 757.1 cm^{-1} arising from =C-H bending or/and C-Cl stretch. Peaks at 1217.6 cm^{-1} and 1361.9 cm^{-1} correspond to the imidazolium ring and the CH_2 vibrational band. The peak at 1529.8 cm^{-1} arises because of C=C stretch, 1471.2 cm^{-1} is from C-H bending, and 1740.5 cm^{-1} mode is from C=O stretch is from the carboxylic acid functional group of citric acid. A peak at 3020 cm^{-1} originates from –N-H stretching, 3453 cm^{-1} is from -OH vibration and 3734.6 cm^{-1} is due to –NH stretching. Distinct changes in the spectra occurred on treatment with citric acid, where changes in the intensity of peaks were observed which established the interaction between the electrode and citric acid. A peak at 983.4 cm^{-1} is due to phosphate symmetric vibration within the ionogel. In the presence of citric acid, there was a major change or stretch in the peaks 1065 cm^{-1}, 788 cm^{-1} and 1361.9 cm^{-1} (Figure 4).

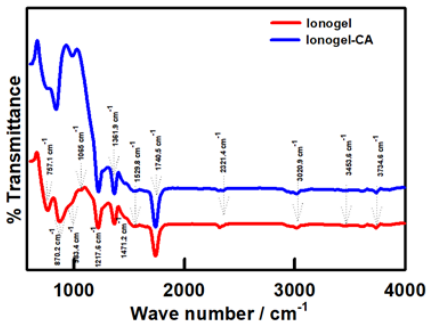

Figure 4 FTIR spectra (a) without and (b) with citric acid.

Citation: Pandey PK, Rawat K, Aswal VK, et al. Hierarchical self-assembly in ionic liquid crosslinked polyelectrolyte gels as a citric acid sensor. *J Appl Biotechnol Bioeng.* 2022;9(5):142–147. DOI: 10.15406/jabb.2022.09.00302

The surface morphology of electrodes without and citric with acid was characterized using scanning electron microscope (SEM) imaging, which is shown in Figure 5a, which clearly reveals branched morphology of ionogel thin film. Image (b) shows surface morphology of electrode with citric acid. This change in surface morphology is caused by the transfer of citric acid to the ionogel interface on the electrode. Detail discussion of analytic detection is given later.

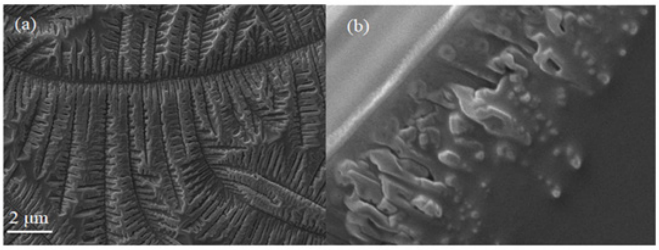

Figure 5 SEM images (a) without and (b) with citric acid.

Optimization of parameters

For the electrochemical sensing of the analytes, a three-electrode cell was operated in the applied potential range of -0.05 to 0.5 V and in each case the redox current flowing in the cell was monitored. The three electrodes used were: DNA ionogel-ITO as working electrode, platinum wire as supplementary electrode and Ag/AgCl as reference electrode. All studies were conducted in standard Zobell's solution (3.3 mM $K_4Fe(CN)_6$, 3.3 mM $K_3Fe(CN)_6$ and 0.1M KCl) medium**.** Scan rate, ionogel concentration and analyte concentration were standardized by repeating the experiments thrice under similar conditions. Initially, we investigated the cyclic voltametric profile of bare ITO, and DNA ionogel-ITO electrode at a fixed scan rate of 50 mV/s in order to understand the electrochemical behavior in Zobell's solution and observed that the peak current of DNA ionogel/ ITO electrode was higher than the blank ITO electrode (Figure 6). This suggested the presence of a film on the ITO surface and there was a reduction in electron transfer accessibility by the gel film compared to ITO electrode.[32,33]

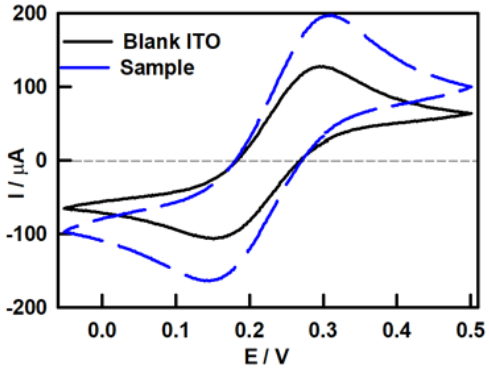

Figure 6 Cyclic voltammetric response of DNA ionogel and bare ITO.

Later, the electrochemical response of DNA ionogel-ITO electrode was monitored systematically in the applied potential range of -0.1 to 0.5 V. As the concentration of IL in the ionogel electrode had a significant effect on the electrochemical properties, we first investigated this by varying IL concentration using peak current as an indicator. Figure 7(a) shows the CV profile of DNA ionogel-ITO electrode with varying IL concentrations. Figure 7(b) shows an increase in the anodic current I_a at IL concentration of 0.7% (w/v) and then it decreases, and remains invariant thereafter. As the highest peak current (I_a, anodic and I_c, cathodic) was obtained at 0.7% IL concentration indicating that this particular concentration had superior electron transfer properties and sensitivity compared to other samples. Therefore, all further experiments were performed using this particular electrode.

The different analytes used in the study were urea (U), oxalic acid (OA), gallic acid (GA), cholesterol (CHOX), Dextrose (DEX), and citric acid (CA). Stock solutions of 10 mM of these analytes were separately prepared in deionized water and stored at 4 ^{0}C when not in use. The electron transfer kinetics of the electrode was analyzed using cyclic voltammetry. Initially, scan rate was optimized prior to performing studies on analytes. Thereafter, electrochemical studies were conducted for different analytes in the concentration range of 0.02-0.20 mM. The electrochemical sensing profile suggested that the DNA ionogel-ITO electrodes were only selective to citric acid (Figure 7).

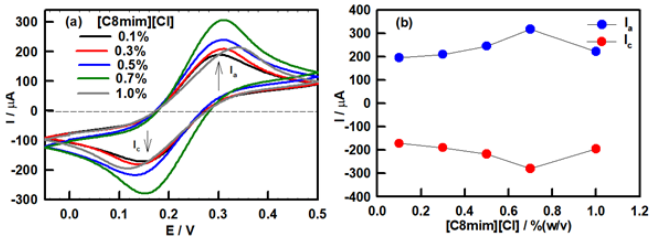

Figure 7 (a) Cyclic voltammetric response of ionogel electrode for different IL concentration varying from 0.1% to 1% (w/v), and (b) Electrode current (I_a and I_c) dependence on IL concentration in the ionogels.

Detection of analytes

The sole objective of the study was to analyse the potential utility of the DNA ionogel electrodes towards bioanalyte detection. We systematically probed the efficacy of these electrodes in the detection of various bioanalytes in the concentration range of 0.02-0.2 mM at a fixed scan rate of 50 mV/s by monitoring the change in the anodic and cathodic peak current. A single DNA ionogel-ITO electrode was used in the whole concentration range of a given analyte to the minimize instrumental error. Distinct changes in CV profiles were observed in the case of citric acid while no significant changes were seen in the case of other analytes. The anodic peak current was observed to increase with concentration of citric acid. Additionally, a shift in the anodic peak current towards higher potential was observed with increase in citric acid concentration. Figure 8a shows the CV response of DNA ionogel-ITO electrode to varying citric acid concentration. It clearly indicates an increase in the oxidation (I_a) and reduction (I_c) current on treatment with citric acid, and thus, infers that the electrocatalytic reaction yielding the redox current was due to the citric acid presence. No change in the peak current was found for all other bioanalytes even at very high concentration of 0.2 mM (data not shown).

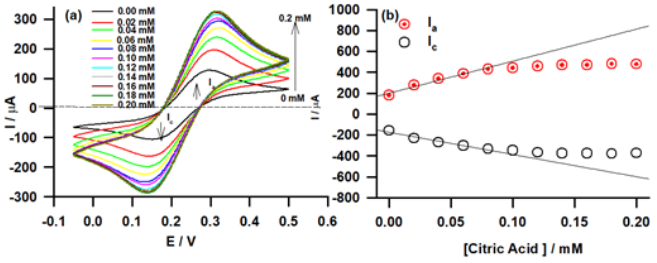

Figure 8 (a) CV response of DNA ionogel electrode to the varying concentration of the citric acid analyte, (b) Linear dependence of redox currents as function of citric acid concentration in the range of 0.02-0.08 mM.

Citation: Pandey PK, Rawat K, Aswal VK, et al. Hierarchical self-assembly in ionic liquid crosslinked polyelectrolyte gels as a citric acid sensor. *J Appl Biotechnol Bioeng.* 2022;9(5):142–147. DOI: 10.15406/jabb.2022.09.00302

Discussion

On plotting the anodic and cathodic peak current for citric acid with respect to its concentration, a linear relationship was observed with a least-square fitting χ^2 value of 0.97 and 0.98, respectively (Figure 8b). The linear detection range was found to be 0.02 to 0.08 mM and the sensitivity of electrode was calculated from the slope of current dependence of ionogel towards citric acid concentration (= 12.25 mA/mM cm^2). Table 1 provides a comparative analysis of the different sensing platforms for citric acid detection and their relative sensitivity, which suggests that the present system offers a very high degree of sensitivity compared to the existing enzymatic and non-enzymatic modes of detection.[33–37]

Table 1 Comparison of different citric acid sensors

S. No.	Composition	Linear range / M	Detection limit / (mol L^{-1})	References
1.	Cobalt(II)–phthalocyanine modified carbon paste electrode	1 0.8–16.6	2.54×10^{-6}	34
2.	Ion chromatography with suppressed conductivity detection	$(10.4\text{-}5205)\times10^{-7}$	3.13×10^{-7}	35
3.	Pyrolysis mass spectrometry	$5.21\times(10^{-8}\text{-}10^{-1})$	5.21×10^{-9}	36
4.	Reagent-injection spectrophotometry	$(3.0 – 600)\times10^{-8}$	3×10^{-8}	37
5. DNA based	Ionogel/ITO	$(0.02\text{-}0.08)\times10^{-3}$	2.4×10^{-4}	[Present Work]

Enzymatic mode detection involving citrate lyase enzyme depends on the catalytic hydrolysis of citric acid. In the present method, a non-enzymatic approach is proposed where changes in electrochemical current were observed when the electrode was treated with increasing concentration of citric acid. Thus, a similar process to that of enzymatic reaction occurs where on interaction with the system, decomposition of citric acid produces oxaloacetate, which subsequently gets converted to COO^-, that is responsible for the increase in peak current. A representative mechanism of citric acid detection by DNA ionogel-ITO electrode is presented in Scheme 1.

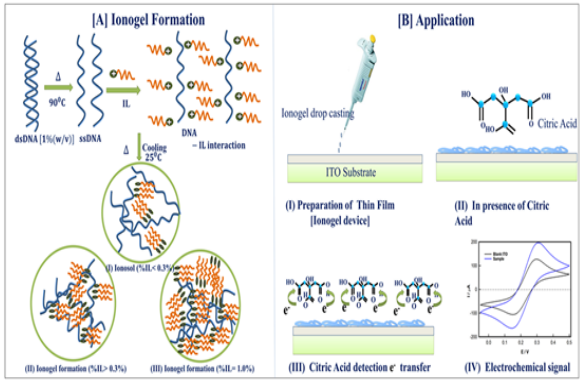

Scheme 1 (A) Gelation of DNA in ionic liquid solution, (B) DNA ionogel/ITO electrode (I) its preparation, (II) electrode in citric acid solution, (III) electron transfer of electrode surface and (IV) typical electrochemical response.

The interference data for citric acid sensor shows that the presence of another analyte do not affect the anode current I_a the sensor. Thus, it can be concluded that the sensor is specific to citric acid in the presence of other analytes of same concentration (Figure 9).

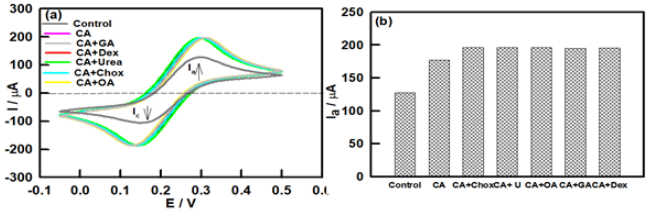

Figure 9 (a) CV response of DNA ionogel-ITO electrode to citric acid in presence interfering analyte. Concentration of citric acid and test analyte were same. (b) Bar diagram showing the effect of other analytes on citric acid sensing.

Conclusion

It has been shown that IL used can cause gelation in DNA solutions. It was noticed from rheology that these ionogels had moderate (10 to 60 Pa) rigidity modulus, but were endowed with tunable gelation temperature (52 to 62 ^{0}C). DNA being a strong polyelectrolyte binds to the positive head group of IL which forms DNA-IL complexes which in turn undergo gelation, because the electrostatic barrier of repulsion between inter DNA strands is depleted. The present study not only focused on the development of DNA ionogel system, but it was also used for the successful detection of citric acid. The electrode exhibited a very high degree of sensitivity of 12.25 mA mM^{-1} cm^{-2} in the linear range of 0.02-0.08 mM. This provides a new platform for the enzyme-free detection of citric acid, and holds promise for real-time use in clinical samples.

Supporting information (SI)

The variation of power-law exponent and viscoelastic length obtained from G0 obtained from frequency sweep rheology data for different samples are included in SI.

Acknowledgments

PKP acknowledge UGC-BSR, Government of India for Senior Research Fellowship. The authors thank the Advanced Instrument Research Facility of the University for TEM facility. KR thanks DST (SERB/EMR/2016/004868), ICMR (35/11/2019-Nano/BMS) and UGC-startup, Government of India for a research grant. This study was funded by DST-Purse II Department of Science and Technology, Government of India (DST), India.

Conflicts of interest

The authors declare no competing interests.

References

1. Cheng E, Xing Y, Chen P, et al. A pH-triggered, fast-responding DNA hydrogel. *Angew Chem.* 2009;48(41):7760–7763.
2. Rosa H, Petri DFS, Carmona Ribeiro AM. Interactions between bacteriophage DNA and cationic biomimetic particles. *J Phys Chem B.* 2008;112(51):16422–16430.
3. Xu Y, Wu Q, Sun Y, et al. Three–dimensional self–assembly of graphene oxide and DNA into multifunctional hydrogels. *ACS Nano.* 2010;12:7358–7362.

4. Li C, Faulkner Jones A, Dun AR, et al. Rapid formation of a supramolecular polypeptide–DNA hydrogel for in situ three-dimensional multilayer bioprinting. *Angew Chem Int Ed.* 2015;54(13):3957–3961.
5. Topuz F, Okay O. Formation of hydrogels by simultaneous denaturation and cross–linking of DNA. *Biomacromolecules*. 2009;10(9):2652–2661.
6. Yang D, Hartman MR, Derrien TL, et al. DNA materials: bridging nanotechnology and biotechnology. *Acc Chem Res.* 2014;47(6):1902–1911.
7. Zinchenko A, Taki Y, Sergeyev VG, et al. DNA–assisted solubilization of carbon nanotubes and construction of DNA–MWCNT cross–linked hybrid hydrogels. *Nanomaterials (Basel)*. 2015;5(1):270–283.
8. Costa D, Miguel MG, Lindman B, et al. Swelling properties of cross–linked DNA gels. *Adv Colloid Interface Sci.* 2010;158(1–2):21–31.
9. Dave N, Chan MY, Huang PJJ, et al. Regenerable DNA–functionalized hydrogels for ultrasensitive, instrument–free mercury (II) detection and removal in water. *J Am Chem Soc.* 2010;132(36):12668–12673.
10. Lee CK, Shin SR, Lee SH, et al. DNA hydrogel fiber with self-entanglement prepared by using an ionic liquid. *Angew Chem Int Ed.* 2008;47(13):2470–2474.
11. Morán MC, Miguel MG, Lindman. DNA gel particles: particle preparation and release characteristics. *Langmuir*. 2007;23(12):6478–6481.
12. Zinchenko A, Miwa Y, Lopatina LI, et al. DNA hydrogel as a template for synthesis of ultra–small gold nanoparticles for catalytic applications. *ACS Appl Mater Interfaces.* 2014;6(5):3226–3232.
13. Orakdogen N, Erman B, Okay O. Evidence of strain hardening in DNA gels. *Macromolecules*. 2010;43(3):1530–1538.
14. Horkay F, Basser PJ. Osmotic observations on chemically cross–linked DNA gels in physiological salt solutions. *Biomacromolecules.* 2004;5(1):232–237.
15. Arfin N, Aswal VK, Kohlbrecher J, et al. Relaxation dynamics and structural changes in DNA soft gels. *Polymer*. 2015;65:175–182.
16. Pandey PK, Rawat K, Aswal VK, et al. Structural hierarchy in DNA hydrogels. *J Appl Biotechnol Bioeng.* 2017;2(4):144–150.
17. Sui X, Hempenius MA, Vancso GJ. Redox–active cross–linkable poly (ionic liquid) s. *J Am Chem Soc.* 2012;134(9):4023–4025.
18. He Y, Li Z, Simone P, et al. Self–assembly of block copolymer micelles in an ionic liquid. *J Am Chem Soc.* 2006;128(8):2745–2750.
19. Pinkert A, Marsh KN, Pang S, et al. Ionic liquids and their interaction with cellulose. *Chem Rev.* 2009;109(12):6712–6728.
20. Pandey PK, Rawat K, Aswal VK, et al. Imidazolium based ionic liquid induced DNA gelation at remarkably low concentration. *Colloids and Surfaces A.* 2018;538:184–191.
21. He Y, Boswell PG, Bühlmann P, et al. Ion gels by self–assembly of a triblock copolymer in an ionic liquid *J Phys Chem B* 2007;111(18):4645–4652.
22. Pandey PK, Rawat K, Aswal VK, et al. DNA ionogel: Structure and self–assembly. *Phys Chem Chem Phys.* 2017;19(1):804–812.
23. Le Bideau J, Viau L, Vioux A. Ionogels, ionic liquid based hybrid materials. *Chem Soc Rev.* 2011;40(2):907–925.
24. Kohlbrecher J, Wagner W. The new SANS instrument at the Swiss spallation source SINQ. *J Appl Crystallogr.* 2000;33:804–806.
25. Aharony A. *Introduction to Percolation Theory*. Taylor & Francis Group; London; 1994.
26. Pandey PK, Rawat K, Aswal VK, et al. DNA ionogel: Structure and self–assembly. *Phys Chem Chem Phys.* 2016;19(1):804–812.
27. Ferry JD. Viscoelastic Properties of Polymers. John Wiley & Sons; 1980.
28. Barnes HA. A Handbook of Elementary Rheology, University of Wales, Institute of Non–Newtonian fluid Mechanics: Aberystwyth. 2000.
29. Ajji A, Choplin L. Rheology and dynamics near phase separation in a polymer blend: model and scaling analysis. *Macromolecules.* 1991;24:5221–5223.
30. Rawat K, Pathak J, Bohidar HB. Effect of persistence length on binding of DNA to polyions and overcharging of their intermolecular complexes in aqueous and in 1–methyl–3–octyl imidazolium chloride ionic liquid solutions. *Phys Chem Chem Phys.* 2013;15:12262–12273.
31. Svintradze DV, Mrevlishvili GM, Metreveli N, et al. Collagen–DNA complex. *Biomacromolecules*. 2008;9:21–28.
32. Joshi N, Rawat K, Solanki PR, et al. Biocompatible laponite ionogels based non–enzymatic oxalic acid sensor. *Sens Bio–Sens Res.* 2015;5:105–111.
33. Kaushik A, Solanki PR, Ansari AA, et al. Iron oxide–chitosan nanobiocomposite for urea sensor. *Sensors and Actuators B: Chemical*. 2009;138:572–580.
34. Nascimento RF, Selva TMG, Ribeiro WF, et al. Flow–injection electrochemical determination of citric acid using a cobalt (II)–phthalocyanine modified carbon paste electrode. *Talanta*. 2013;105:354–359.
35. DeBorbaa BM, Rohrera JS, Bhattacharyya L. Development and validation of an assay for citric acid/citrate and phosphate in pharmaceutical dosage forms using ion chromatography with suppressed conductivity detection. *J Pharm Biomed Anal.* 2004;36:517–524.
36. Ghassempour A, Najafi NM, Amiri AA. Determination of citric acid in fermentation media by pyrolysis mass spectrometry. *J Anal Appl Pyrolysis.* 2003;70:251–261.
37. Themelis DG, Tzanavaras PD. Reagent–injection spectrophotometric determination of citric acid in beverages and pharmaceutical formulations based on its inhibitory effect on the iron (III) catalytic oxidation of 2, 4–diaminophenol by hydrogen peroxide. *Anal Chim Acta.* 2001;428:23–30.